Comparison of several advanced oxidation processes for the decolorization of Reactive Red 120 azo dye in aqueous solution

Erdal Kusvuran [a,*], Osman Gulnaz [b], Sibel Irmak [a], Osman M. Atanur [a],
H. Ibrahim Yavuz [a], Oktay Erbatur [a]

[a] *Chemistry Department, Arts and Sciences Faculty, Cukurova University, 01330 Balcali, Adana, Turkey*
[b] *Biology Department, Arts and Sciences Faculty, Cukurova University, 01330 Balcali, Adana, Turkey*

Abstract

In this study UV/TiO$_2$, electro-Fenton (EF), wet-air oxidation (WAO), and UV/electro-Fenton (UV/EF) advanced oxidation processes (AOPs) have been applied to degrade Reactive Red 120 (RR120) dye in aqueous solution. The most efficient method on decolorization and mineralization of RR120 was observed to be WAO process. Photocatalytic degradation of RR120 by UV/TiO$_2$ have been studied at different pH values. At pH 3 photocatalytic degradation kinetics of RR120 successfully fitted to Langmuir–Hinshelwood (L–H) kinetics model. The values of second order degradation rate (k'') constant and adsorption constant (K) were determined as 4.525 mg L^{-1} min^{-1} and 0.387 L mg^{-1}, respectively. Decolorization efficiency observed in the order of WAO > UV/TiO$_2$ = UV/EF > EF while WAO > UV/TiO$_2$ > UV/EF > EF order was observed in TOC removal (mineralization). For all AOPs, it was found that degradation products in reaction mixture can be disposed safely to environment after 90 min treatment.
© 2004 Elsevier B.V. All rights reserved.

Keywords: Reactive red 120; Advanced oxidation processes; L–H kinetics; Decolorization; Mineralization

1. Introduction

The studies have showed that toxic and refractory organics including dyes in wastewater could be destroyed by most advanced oxidation processes (AOPs). As one of AOPs photocatalytic treatment of wastewater is an emerging technology. In this process the solution is illuminated with UV irradiation in the presence of a suitable photocatalyst, mainly TiO$_2$. The use of TiO$_2$ as photocatalyst for environmental clean-up has been of great interest due to its high efficiency, photochemical stability, non-toxic nature and low cost when sunlight is used as the source of irradiation. This method was successfully applied to the decomposition of many organic contaminants, i.e. including azo dyes [1–4] and other dyes [5,6]. The basic principles of photocatalysis over illuminated TiO$_2$ are well established [7–9]. In the oxidation with TiO$_2$, photo-excitation with light of energy greater than the TiO$_2$ bandgap promotes an electron from the valance band to the conduction band, and leaves an electronic vacancy or hole (h$^+$) in the valance band. The highly oxidative h$^+$ ($E^\circ = +2.7$ V) may directly react with the surface-sorbed organic molecules [10] or indirectly oxidize the organic compounds via formation of OH$^\bullet$ radicals.

The other advanced oxidation process is electro-Fenton (EF). In this method, OH$^\bullet$ radicals are produced in the bulk of the solution in the presence of Fe^{2+}. Hydrogen peroxide is produced electrochemically upon reduction of oxygen on several electrodes (mercury pool, graphite, carbon-polytetrafluoroethylene O$_2$-fed cathodes). Reaction pathways of production of OH$^\bullet$ radicals electrochemically can be represented with the reactions given below:

$$Fe^{3+} + e^- \rightarrow Fe^{2+} \tag{1}$$

$$O_2 + 2e^- + 2H^+ \rightarrow H_2O_2 \tag{2}$$

$$Fe^{2+} + H_2O_2 \rightarrow Fe^{3+} + OH^\bullet + OH^- \tag{3}$$

OH$^\bullet$ is a non-selective, very powerful oxidizing agent that reacts with organics yielding dehydrogenated or hydroxylated derivatives, until their mineralization (conversion into CO$_2$ and inorganic ions) is achieved. In this system catalytic

* Corresponding author. Tel.: +90-322-338-6540;
fax: +90-322-338-6070.
E-mail address: erdalkusvuran@yahoo.com (E. Kusvuran).

reaction can be propagated via Fe^{2+} regeneration which mainly takes place by the reduction of Fe^{3+} species with electrogenerated H_2O_2. H_2O_2 is produced via reaction (2) by bubbling O_2 gas through the acidic solution with a small concentration of Fe^{2+} or Fe^{3+} in the cathodic compartment. The pollutants are destroyed by the action of $OH^\bullet$ formed in reaction (3). This system has been used successfully for the hydroxylation of some organic compounds [11–13].

Wet-air oxidation (WAO) is another effective method and extensively used in industrial oxidation process to treat of hazardous wastes and heavily polluted effluents [14,15]. The basic idea of WAO [16] is that oxygenation of organic and/or oxidizable inorganic containing matters in the fluid phase to inorganic matters or small molecular organic matters using air or pure oxygen as oxidant at upper temperatures (125–350 °C) and pressures (0.5–20 MPa) [17]. The first patent of WAO was forward by Strehlenert in 1911 [18]. When WAO process compared with ozone or hydrogen peroxide, molecular oxygen exhibits low reactivity in water, which requires several operation conditions [19]. In WAO processes elevated temperatures and pressures increase the concentration of dissolved oxygen [20] and enhance the contact between the molecular oxygen and organic matter [21] and thus the oxidation rate. Although the degree of oxidation in the process depends upon the process conditions, retention time and feed composition also affect the performance of the process [22]. WAO process can treat any kind of organic aqueous waste and domestic sludge, even those produced by various branches of industrial activity with lower secondary pollution and higher reaction rate. This process can be coupled with a biological treatment facility to eliminate the sludge [21–24]. Unlike incineration which is handicapped by its bad ecological image this process has very limited interaction with the environment. This technique requires high first investment capital but the operating cost is lower than the other chemical and biological techniques.

The organic dyes are large group of pollutants in waste-waters originating from textile and related industries. Color removal from this kind of effluents has been a matter of considerable interest because of their toxicity and/or refractory nature. Advanced oxidation processes extensively studied in this field because they can provide the ultimate solution for the destruction of commercial dyes in wastewater. The toxicity of dye intermediates formed during the AOP applications play a crucial role in dye decolorization and degradation. Therefore, after effective elimination of the pollutants the effluent has to be tested for toxicity. The aim of this study was to investigate the decolorization and mineralization rate of Reactive Red 120 dye (RR120), which is a component of azo dyes group by using UV/TiO_2, EF, UV/EF, and WAO advanced oxidation processes. After each treatment, the solution was controlled if it is safely disposable to environmental receiving bodies.

2. Materials and method

2.1. UV/TiO_2 experiments

Reactive Red 120 dye (RR120) was purchased from Ak Kim Ltd., Gaziantep, Turkey (Fig. 1) and used without further purification. Titanium dioxide used was anatase (Aldrich, 99.9+% pure). The light source used was the mercury vapor UV lamp (UVP-CPQ-7871), which emits its max radiation at 254 nm. The intensity of the incident light inside the photo reactor was measured as 0.50×10^{-6} einstein s^{-1} by uranil actinometer method [25].

The solutions of RR120 were prepared at different initial concentrations (20–100 mg L^{-1}) and necessary pH adjustments were made with 0.1 M H_2SO_4 and 0.1 M NaOH. Before adjustment pHs of the 20 and 100 mg L^{-1} RR120 solutions were determined to be 6.30 ± 0.05 and 6.60 ± 0.05, respectively. The solution was placed in the 220 mL reaction tube (pyrex) and mixed with 0.5 g L^{-1} titanium dioxide powder and sonicated in ultrasonic bath (Lab-line instruments 9314-1) to disperse TiO_2 uniformly in the solution. During the runs oxygen gas with 0.35 L min^{-1} flow rate was continuously bubbled into dispersion. One milliliter of sampling was carried out at 0, 10, 20, 30, 40, 50, and 60 min of cumulative irradiation times. The samples were centrifuged and analyte concentration in centrifugate was analyzed by Shimadzu UV-2101 PC Scanning spectrophotometer at 509 nm.

2.2. Adsorption tests in the dark

The adsorption isotherm of RR120 on TiO_2 surface was determined by mixing 50 mL aqueous solution of the dye at various initial concentrations at pH 3 for 30 min in a mechanical shaker. The extend of adsorption of the azo dye on TiO_2 was evaluated in terms of color removal rate (absorbance at 509 nm). Data obtained from the adsorption experiments of RR120 were fitted to the modified empirical
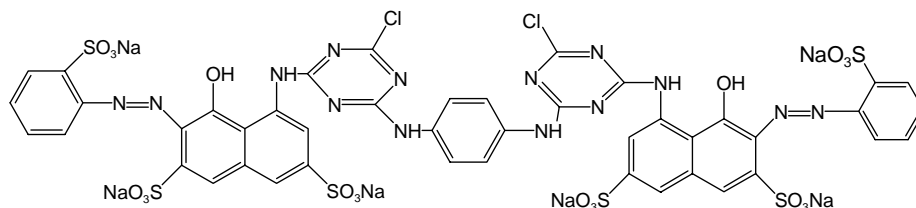

Fig. 1. Chemical structure of RR120.

Langmuir equation [26,27]:

$$\frac{C_e}{Q_e} = \frac{1}{K_L} + \frac{a_L}{K_L} C_e$$

where C_e is the equilibrium concentration of RR120 after 30 min; Q_e the adsorbed dye concentration on TiO_2 surface. K_L and a_L are isotherm constants for particular solute–solvent combination. The dimensionless separation factor (R_L) indicates the shape of the Langmuir isotherm to be either favorable ($0 < R_L < 1$), unfavorable ($R_L > 1$), linear ($R_L = 1$), or irreversible ($R_L = 0$):

$$R_L = \frac{1}{1 + KC_0}$$

C_0 in the equation is the highest initial dye concentration ($mg\,L^{-1}$).

2.3. Electro-Fenton experiments

$Fe(NH_4)_2(SO_4)_2\cdot6H_2O$ and Nafion 117 used in EF experiments were purchased from Aldrich. Graphite felt (RVG 2000) was from Carbone Loraine. Electrolytic experiments were conducted in a 300 mL glass reactor. The platinum gauze anode was separated from the cathode part by using Nafion 117 membrane. The carbon felt ($3\,cm \times 5\,cm$) was used as the working electrode (cathode). Saturated calomel electrode was used throughout the electrolytic experiments as the reference electrode. Controlled potential electrolysis and coulometric measurements were performed by an EG&G Par model 273 A electrochemical system. In a typical electrolytic experiment, following the addition of the metal salt into pH 3 solution of RR120, O_2 gas was bubbled through the solution for 20 min and then -0.55 V/SCE constant cathodic potential was applied to the system while O_2 gas bubbling was continued throughout the electrolysis. Fe^{2+}/RR120 = 3 (mol/mol) ratio was used for all EF experiments. Predetermined amounts of aliquots were withdrawn from the system at certain time intervals. Each aliquot of solution that was withdrawn from the system had been analyzed immediately by UV spectrophotometer.

2.4. Wet-air oxidation experiments

Oxidation of RR120 solutions was carried out in the high pressure Hastelloy reactor (4740 Series, Parr Instrument, USA) that has an effective volume of 71 mL. The gas inlet, pressure gauge and on–off Hoke valve were mounted on the top of the head. The connection of the system elements was made with 0.25 in. O.D. tubing.

The operating pressure of the oxidation reaction was controlled by a gauge above the head of reactor. Bottled oxygen was used as the oxygen supply for the oxidation reaction. The oxygen partial pressure was kept at 17 bar in all experiments. Desired reaction temperature was provided by heating the reactor in a eutectic salt bath whose components were 53% KNO_3, 40% $NaNO_2$, and 7% $NaNO_3$. The temperature

was controlled by PID heat controller (Elimko, Turkey) to keep temperature of salt solution with in $\pm3\,°C$ of set point.

In a typical WAO experiment, 50 mL of the RR120 dye solution was placed into the reactor. After the reactor was sealed it was pressurized by supplying oxygen gas and heated to the desired temperature by immersing into the eutectic salt bath. The operating temperature was varied between 200 and 300 °C. The oxidation reactors were agitated by a shaker in eutectic salt bath at 150 cycles/min. Because of batch type, the reactor does not allow to sampling for analysis at various time intervals. Therefore, the experiments were repeated at various time intervals for all temperatures. At a certain reaction time, the reactor was cooled rapidly up to room temperature; gas effluent depressurized slowly and reactor was unsealed. The solution of this experiment was one sampling. WAO runs were carried out at three different temperatures (200, 250 and 300 °C) at various reaction times. The solutions were analyzed by UV-Visible spectrophotometer and TOC analyzer.

2.5. Mineralization of the RR120 solutions during AOPs

Mineralization of the RR120 solutions during AOPs treatment was followed by measuring the total organic carbon contents using Tekmar Dohrmann Apollo 9000 instrument. In a typical application, an aliquot of 10 mL was withdrawn from the reaction medium at certain intervals. In electro-Fenton application, 10 mL solution was filtered through glass frit to get rid of carbon contamination from the carbon felt which was used as electrode in electrolytic experiments. In UV/TiO_2 application, 10 mL solution was centrifuged at 4000 rpm to get rid of particular TiO_2 contamination. The samples were ignited at 700 °C on platinum-based catalyst, and the carbon dioxide formed was swept by pure oxygen as the carrier gas through a nondispersive infrared (NDIR) detector.

2.6. Toxicity test

The *Pseudomonas putida* growth inhibition test was performed according to the procedures described in the ISO (ISO, 1995) protocol [28]. The inhibiting effect of RR120 degradation products at a certain time was determined by the increase of turbidity of bacterial cultures. The mineral medium composed for the test was as follows ($mg\,L^{-1}$): $NaNO_3$ 125; K_2HPO_4 30; KH_2PO_4 15; D (+) glucose monohydrate 500; $MgSO_4\cdot7H_2O$ 50 and iron (III) citrate 0.0125. The pH was adjusted to 7.4 ± 0.1. The mineral medium was mixed with the sample at each oxidation time. The result was compared with the turbidity of the control culture incubated under the same conditions, but without the RR120 degradation products, after a 18 ± 1 h incubation duration at $26 \pm 1\,°C$. Turbidity measurement of the bacterial biomass grown in the samples was performed on a Shimadzu UV-2101 PC scanning spectrophotometer at 600 nm. Toxicity test experiments for each applied methods were run in

three replicates. The percentage of cell multiplication inhibition was calculated in conformity with the ISO standard (ISO, 1995) for all samples.

3. Results and discussion

3.1. UV/TiO$_2$

3.1.1. The effect of pH on photocatalytic decolorization of RR120

The experiments were carried out with $40 \, \text{mg} \, \text{L}^{-1}$ dye concentration at pH 3, 5, 7, and 9 for 30 min reaction time (Fig. 2). Decomposition of RR120 was obtained under 40% level at each pHs for 30 min illumination time. Maximum decomposition with 90% was observed at pH 3. Degradation of organic compounds exhibited different behaviors depending on pH studied [29–31]. The zero point charge pH (pH$_{\text{zpc}}$) for anatase TiO$_2$ used in this study was around pH $\approx$ 4 [31,32]. Therefore, catalyst surface was positively charged at acidic medium and negatively at basic medium. Repulsions between same charged TiO$_2$ surfaces prevent the agglomeration of the catalyst. It was observed that increasing pH of the solution resulted decrease of the decolorization rate of RR120. Since the dye has sulfonate groups in its structure, which are negatively charged, the acidic solution favors adsorption of the dye onto TiO$_2$ surface. Thus, decolorization efficiency increased. At this pH, there is also formation of OH$^\bullet$ radicals which react with dye molecules and increase the decolorization level. As the pH of the solution is increased, the adsorption of dye molecules onto catalyst surface decreased. Therefore, decolorization level was observed to be low at basic pH medium. Similar results have been reported for photocatalytic oxidation of some azo dye pollutants [1,33]. At pH 5, TiO$_2$ particle surfaces should mainly be neutral. This probably causes agglomerization of TiO$_2$ catalyst. As a result of that, decomposition of dye at this pH was observed to be lower than at those of pH 7 and 9 after 15 min reaction time. The
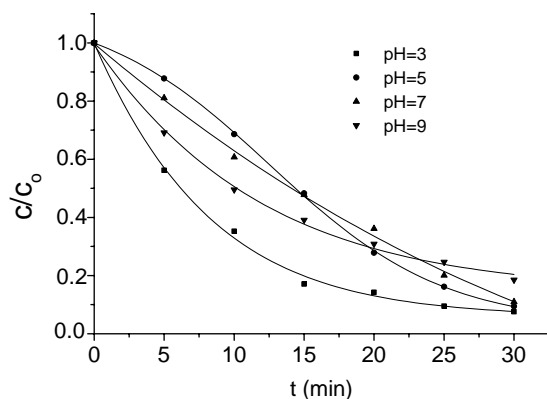

Fig. 3. Degradation of RR120 in solutions of various initial concentrations by UV/TiO$_2$ application (pH 3, TiO$_2$ = $0.5 \, \text{g} \, \text{L}^{-1}$, O$_2$ = $0.5 \, \text{L} \, \text{min}^{-1}$).

similar result was observed for pH 7 after 20 min reaction time.

3.1.2. Photocatalytic degradation of RR120

The degradation experiments of RR120 were carried out with 20, 40, 60, 80, and $100 \, \text{mg} \, \text{L}^{-1}$ initial concentrations at pH 3. Fig. 3 shows the decolorization of RR120 at different initial dye concentrations with varying illumination time. It is observed that the more diluted was the initial solution, the faster was the degradation. For instance, at $20 \, \text{mg} \, \text{L}^{-1}$ initial concentration all $20 \, \text{mg} \, \text{L}^{-1}$ dye solution has been degraded after 20 min reaction time. The respective value at $100 \, \text{mg} \, \text{L}^{-1}$ initial concentration is $71.4 \, \text{mg} \, \text{L}^{-1}$. The amount of photoactive sites on TiO$_2$ surface have decreased due to adsorption of the organic compound and its degradation products in concentrated solutions. Therefore, degradation rate has decreased [29,33,34].

The Langmuir–Hinshelwood (L–H) model was used to analyze the photooxidation kinetics of dye. In photocatalytic oxidation process, adsorption has been considered to be critical in heterogeneous photocatalytic oxidation. The kinetics L–H model which was modified by Heredia et al. [35] was fitted to our results. According to L–H kinetics second order decomposition rate of organic compound may be expressed as:

$$r = k' \Phi_{\text{OH}} \Phi_{\text{OC}}$$

In this equation k' is the surface second order rate constant, Φ_{OH} and Φ_{OC} are the fractions of sites covered by hydroxyl radicals and organic compounds, respectively. Second order kinetics equation can be written in terms of a pseudo-first order kinetic constant as follows [35]:

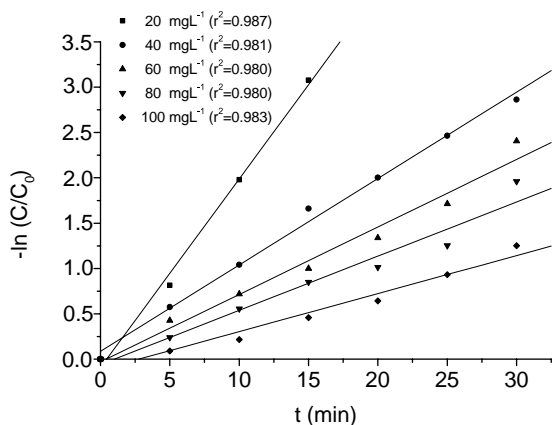$$\frac{1}{k_{\text{obs}}} = \frac{1}{k'' K} + \frac{C_0}{k''}$$

Fig. 2. UV/TiO$_2$ photocatalytic degradation of RR120 at various pHs (C_0 = $40 \, \text{mg} \, \text{L}^{-1}$, TiO$_2$ = $0.5 \, \text{mg} \, \text{L}^{-1}$).

Fig. 4. Linear transforms $-\ln C/C_0$ vs. time for the decomposition of RR120 during UV/TiO$_2$ application.

Table 1
Pseudo-first order rate constants and half-life of RR120 during various AOPs

AOPs methods	First order, k_{obs} (min^{-1})	$t_{1/2}$ (min)
UV/TiO$_2$		
20 mg L^{-1}	0.208	3.3
40 mg L^{-1}	0.095	7.3
60 mg L^{-1}	0.074	9.3
80 mg L^{-1}	0.060	11.6
100 mg L^{-1}	0.042	16.5
EF		
20 mg L^{-1}	0.200	3.5
40 mg L^{-1}	0.071	9.7
60 mg L^{-1}	0.063	11.0
80 mg L^{-1}	0.060	11.5
100 mg L^{-1}	0.058	11.9
WAO		
300 °C	0.334	2.1
250 °C	0.165	4.2
200 °C	0.035	19.6

where k_{obs} is pseudo-first order kinetic constant, k'' a second order rate constant, and K the adsorption constant. When initial concentrations are plotted versus $1/k_{obs}$, the rate constant and the adsorption equilibrium constant can be calculated. Kinetics of RR120 was analyzed using $-dc/dt = k_{obs}.C$ kinetic equation. Pseudo first-order rate constants were calculated from slope of plot of $\ln(C/C_o)$ versus time for each compound (Fig. 4).

Fig. 5 shows our results in which plot of $1/k_{obs}$ versus C_0 forms a straight line according to the modified L–H model with the regression coefficient of 0.978. The second order rate constant (k'') and adsorption constant (K) were calculated as 4.525 mg L^{-1} min^{-1} and 0.387 L mg^{-1}, respectively.

Half-life ($t_{1/2}$) and pseudo first order kinetic rate constants with various initial concentrations of RR120 are given in Table 1. The oxidation rate constants have decreased due to increased adsorption constant. The values of half-life for RR120 depending on initial concentrations ranged between 3.3 and 16.5 min. The pseudo-first order rate constants were in 0.208–0.042 min^{-1} range. Larger amounts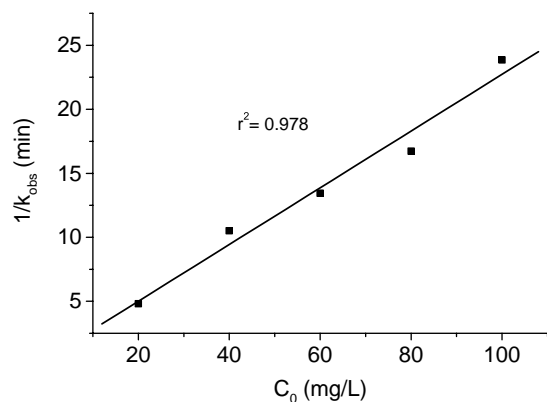 of dye molecules and also their degradation products formed during the application were adsorbed onto the photocatalyst surface at higher initial dye concentrations. They competed with OH$^-$ and H$_2$O for photoactive semiconductor surface sites. This results decreases in the pseudo-first order rate constants via inhibiting the heterogeneous photocatalytic reaction seriously [29,35].

3.2. Adsorption of RR120 on TiO$_2$ in the dark

C_e/Q_e versus C_e plot and Langmuir parameters obtained from this plot are shown in Fig. 6. Langmuir adsorption constant, K_L, and the separation factor, R_L, were calculated as 0.148 L mg^{-1} and 0.064, respectively. From the data in Fig. 6 it is seen that adsorption constant of various initial concentrations of RR120 on TiO$_2$ at pH 3 was almost half of K, which was calculated, by using the kinetic model. The dimensionless separation factor (R_L) indicates that the shape of the Langmuir isotherm was favorable since $0 < R_L < 1$ [36].
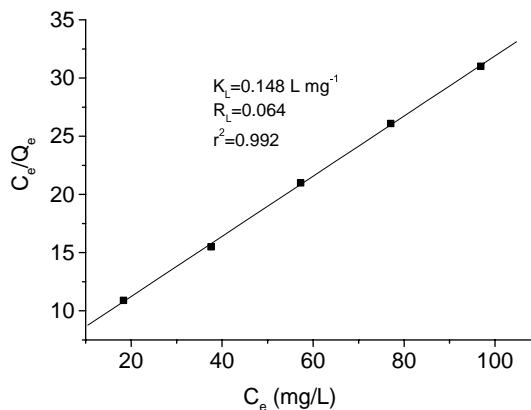

Fig. 5. Determination of the adsorption equilibrium constants and second order rate constants for the adsorption of RR120 on TiO$_2$.

Fig. 6. Establishment of Langmiur monolayer adsorption constant for the adsorption of RR120 on TiO$_2$ at pH 3.
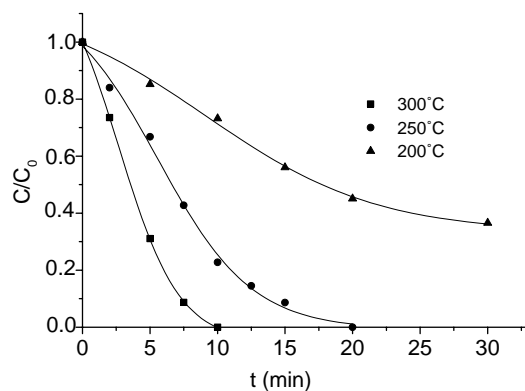
Fig. 7. Decolorization of RR120 at various operation temperatures ($C_0 = 40$ mg/mL, $P_{O_2} = 17$ bar).

Fig. 8. Decolorization of RR120 in various aqueous solutions of different initial concentrations by EF application.

3.3. Decolorization of RR120 by wet-air oxidation

The most important parameter in WAO treatment process is temperature. The effect of temperature on the decomposition of RR120 dye is demonstrated in Fig. 7. The decomposition of RR120 has been improved markedly by increasing the temperature from 200 to 300 °C. It can be seen that RR120 was easily oxidized at 250 °C and 17 bar. The substrate was completely removed after the 20 min treatment in this reaction medium.

The temperature has been the major effect on the reaction rate and half-life ($t_{1/2}$) of the organics [37]. With increasing temperature from 200 to 300 °C, $t_{1/2}$ was decreased from 19.6 to 2.1 min. When the temperature was enhanced by 50 °C, which is from 200 to 250 °C, $t_{1/2}$ had decreased from 19.6 to 4.2 min. When temperature was increased with the same magnitude again, which was from 250 to 300 °C, $t_{1/2}$ had decreased from 4.2 to 2.1 min.

3.4. Decolorization of RR120 by electro-Fenton application

All acidic RR120 solutions tested for different initial concentrations underwent a progressive depollution with increasing electrolysis time. Fig. 8 shows the comparative decolorization of 250 mL solutions of various initial concentrations of RR120 (20–100 mg L^{-1}) at pH 3.0 under -0.55 V/SCE constant cathodic potential applied to the system at 30 °C for 30 min. As can be seen, a reversed proportion was observed between initial concentrations of RR120 and decolorization rates (Table 1). Decolorization rate decreased from 0.200 to 0.058 mg L^{-1} min^{-1} with increasing initial concentration from 20 to 100 mg L^{-1}. After 30 min EF treatment, RR120 was decomposed completely in the solution of 20 mg L^{-1} initial concentration. In solutions of 60, 80, and 100 mg L^{-1} initial concentrations decolorizations were only between 75 and 85% level. $t_{1/2}$ of RR120 decomposition at various initial concentrations increased with increasing initial concentration. When initial concentration
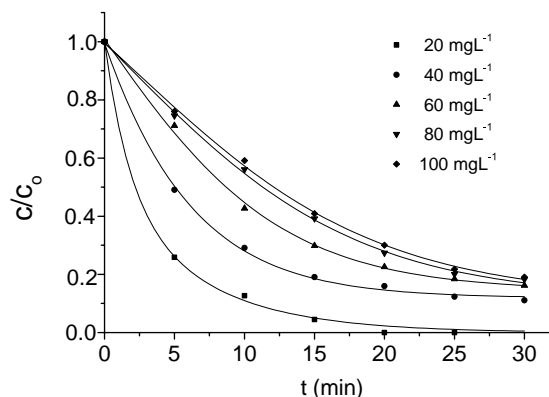
increased from 20 to 40 mg L^{-1} $t_{1/2}$ was increased from 3.5 to 9.7 min. While the initial concentration had doubled, $t_{1/2}$ increased 2.7 times of the initial value. $t_{1/2}$ was almost constant ($\approx$11 min) at higher initial concentrations. The consumed charges for decolorization of RR120 during 30 min electro-Fenton treatment were calculated as 0.55, 0.58, 0.62, 0.67, and 1.23 mF for 20, 40, 60, 80, and 100 mg L^{-1} initial concentration solutions, respectively.

3.5. Comparison of efficiencies of AOPs for decolorization of RR120

In this section, the efficiencies of decomposition of RR120 (40 mg L^{-1}) were investigated by using UV/TiO$_2$, EF, UV/EF, and WAO treatment methods (Fig. 9). All AOPs except WAO process were exhibited nearly the same efficiency on the decomposition of RR120. Degradation levels for these applications were observed in 85–90% range for 30 min treatments. When UV light was used with EF process (UV/EF) degradation of RR120 was observed 5% higher than EF. The most efficient method for decolorization of RR120 was found to be WAO oxidation process. In this process, RR120 was decomposed 100% at even shorter reaction time (20 min at 250 °C). Finally,
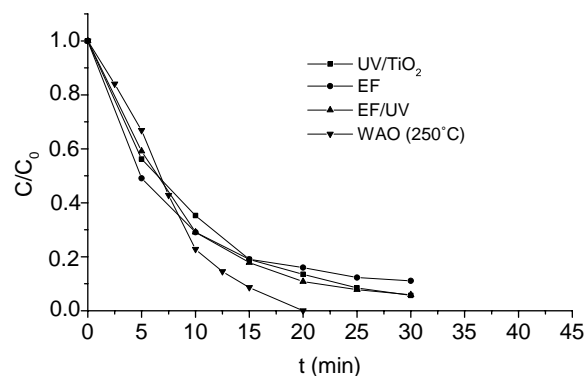

Fig. 9. Decolorization of RR120 aqueous solutions by various AOPs (RR120 = 40 mg L^{-1}).
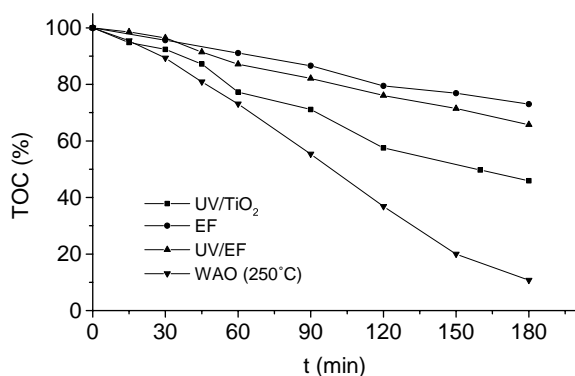
Fig. 10. TOC decreases of RR120 aqueous solutions during various AOP applications ($C_0 = 100\,\mathrm{mg\,L^{-1}}$).

Fig. 11. Bacterial inhibition of intermediates produced during various AOP applications.

degradation efficiency of RR120 was observed to be in the order of, WAO > UV/EF = UV/TiO$_2$ > EF.

3.6. Mineralization of RR120 using different AOPs

Mineralization of RR120 solutions ($C_0 = 100\,\mathrm{mg\,L^{-1}}$) are also followed by measuring the total organic carbon (TOC) contents of the sample solutions withdrawn during the oxidation process. Fig. 10 represents the decrease of TOC percent versus time for different AOPs.

As can be seen, the most effective mineralization was obtained with WAO process (90% mineralization) when 250 °C temperature was applied for RR120 oxidation. The mineralization obtained with other AOPs; UV/TiO$_2$, EF, and UV/EF were 52% or less at the end of 180 min treatment (Fig. 10). The lowest mineralization (24%) was observed in EF application. Despite the presence of UV light (254 nm) the mineralization was not favored with high level in UV/EF process (30% mineralization). UV/TiO$_2$ process was observed to be the second efficient method for mineralization of RR120. Fifty two percent of mineralization was achieved in this method.

The fast removal of RR120 was accompanied by slower TOC reduction indicating that stable intermediates had been formed. Although WAO was observed to be the most effective method complete mineralization was not achieved at the end of the 180 min treatment. Some researchers observed similar results for WAO process, i.e. even at 300 °C, organic materials were not completely mineralized because recalcitrant structural compounds such as acetic acid were formed [23]. In other AOPs although degradation rates were high in 30 min (dye solution turned to colorless) (Fig. 9) the mineralization in these processes was observed in low levels.

Graphite structure is composed of unsaturated aromatic rings which may be active for reacting OH$^{\bullet}$ radicals. Graphite felt, which was used as a working electrode (cathode) in EF application might reduce the degradation efficiency via competing RR120 molecules for reacting with OH$^{\bullet}$ radicals. Even OH$^{\bullet}$ radicals which might have been produced excessively in EF system, important part of
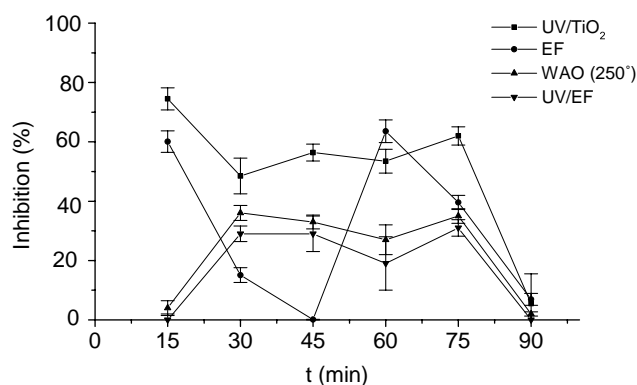
the radicals were consumed by graphite felt. Therefore, the degradation level of TOC in EF and UV/EF processes was observed to be lower than the others.

3.7. Comparison of the toxicity for degradation products of RR120 by using AOPs

In this section of study, the toxicity of intermediates which were formed via decomposition of RR120 with each AOP application were investigated. The toxicity of the original solution ($t = 0$ min) was determined as zero. No bacterial growth inhibition was observed following 90 min treatments in all AOP applications (Fig. 11). Since bacterial inhibition change trends for the AOP applications were quite different, RR120 might have been degraded with different mechanisms (Fig. 11). In WAO and UV/EF processes, inhibition levels obtained due to the new products formed following degradation of RR120 exhibited similar behaviors. The intermediates of both processes during the first 15 min resulted no inhibition and after 30 min, inhibition were increased up to 35% and 30% for WAO and UV/EF, respectively. The inhibition was almost constant at this level for both of the AOPs until 75 min treatments and then further treatment decreased the inhibition to zero level (90 min). Therefore, there wouldn't be any risk when solutions of RR120 which have been treated with these two methods for 90 min would be disposed to the appropriate environmental receiving bodies. The intermediates obtained during TiO$_2$ and EF applications in the first 15 min showed inhibitions of 75% and 60%, respectively. The toxicity was constant about 50% for UV/TiO$_2$ process during treatment upto 75 min. The EF process exhibited different toxicity from the other methods during treatment for degradation of RR120. Especially, toxicity was decreased to zero at 45 min treatment duration and then increased up to 65% level sharply at the end of 60 min treatment, and then began to decrease down to zero level following 90 min treatment. After this point toxicity level was constant at zero level. The final solutions following 90 min treatments were all disposable safely to environmental bodies. Overall, it can be concluded that different methods

resulted in different intermediates since toxicity patterns for the applied treatments were substantially different.

4. Conclusion

In this experimental work, degradation of RR120 dye has been investigated by using several advanced oxidation processes. Among all applied processes wet-air oxidation process was found to be the most effective method. In this process pseudo-first order degradation rate constants have been determined to increase from 0.035 to 0.334 min^{-1} when the temperature was increased from 200 to 300 °C. In this process 90% of TOC removal has been observed at 250 °C following 180 min treatment.

UV/TiO$_2$ was found to be second effective process on mineralization of RR120. 52% of TOC removal was achieved by this process. Decolorization of RR120 by UV/TiO$_2$ process was observed to be optimum at acidic pH. Since the positively charged surfaces repel each other, the possibility of agglomeration is very low at this pH. Even supported with UV light, mineralization by EF process was observed to be very low.

It has been determined that final solutions of AOP applications after 90 min treatment were disposable safely to environment.

Considering the economical aspects, the use of advanced oxidation processes alone are not cheap technologies. For example, even WAO process was found to be the most efficient technique for decolorization of RR120 it is not advisable because of high capital and operating cost. Therefore, these methods must be optimized by adjusting process conditions and/or coupled with another economically feasible method such as biological treatment. Much attention on toxicity of intermediates formed during the AOPs application should be paid in order to determine whether the decolorization or degradation process is biologically and economically feasible. The toxicity and the refractory nature of the pollutant can be reduced up to a certain level and then biological treatment may follow-up.

References

[1] W.Z. Tang, H. An, UV/TiO$_2$ photocatalytic oxidation of commercial dyes in aqueous solutions, Chemosphere 31 (1995) 4157–4170.

[2] Z. Haoqiang, T. He, Photocatalytic Degradation of acid azo dyes in aqueous TiO$_2$ suspension I, The effect of substituents. Dyes Pigments 37 (1998) 231–239.

[3] C. Hu, Y. Tang, J.C. Yu, P.K. Wong, Photocatalytic degradation of cationic blue X-GRL adsorbed on TiO$_2$/SiO$_2$ photocatalyst, Appl. Catal. B 40 (2003) 131–140.

[4] C.G. Silva, J.L. Faria, Photochemical and photocatalytic degradation of an azo dye in aqueous solution by UV irradiation, J. Photochem. Photobiol. A 155 (2003) 133–143.

[5] D. Chatterjee, A. Mahata, Demineralization of organic pollutants on the dye modified TiO$_2$ semiconductor particulate system using visible light, Appl. Catal. B 33 (2001) 119–125.

[6] S. Horikoshi, H. Hidaka, N. Serpone, Environmental remediation by an integrated microwave/UV-illumination method. 1. Microwave-assisted degradation of Rhodamine-B dye in aqueous TiO$_2$ dispersions, Environ. Sci. Technol. 36 (2002) 1357–1366.

[7] M.A. Fox, M.T. Dulay, Heterogeneous photocatalysis, Chem. Rev. 93 (1993) 341.

[8] C. Galindo, P. Jacques, A. Kalt, Photochemical and photocatalytic degradation of an indigoid dye: a case study of acid blue 74 (AB74), J. Photochem. Photobiol. A 141 (2001) 47–56.

[9] C.S. Turchi, D.F. Ollis, C.S. Turchi, D.F. Ollis, Photocatalytic degradation of organic water contaminants: mechanisms involving hydroxyl radical attack, J. Catal. 122 (1990) 178–192.

[10] J. Gimenez, D. Curco, P. Marco, Reactor modelling in the photocatalytic oxidation of wastewater, Water Sci. Technol. 35 (1997) 207–213.

[11] B. Gozmen, M.A. Oturan, N. Oturan, O. Erbatur, Indirect electrochemical treatment of bisphenol A in water via electrochemically generated Fenton's reagent, Environ. Sci. Technol. 37 (2003) 3716–3723.

[12] E. Brillas, J.C. Calpe, J. Casado, Mineralization of 2,4-D by advanced electrochemical oxidation processes, Water Res. 34 (2000) 2253–2262.

[13] B. Boye, M.M. Dieg, E. Brillas, Anodic oxidation, electro-Fenton and photoelectro-Fenton treatments of 2,4,5-trichlorophenoxyacetic acid, J. Electroanal. Chem. 557 (2003) 135–146.

[14] R. Robert, S. Barbati, N. Ricq, M. Ambrosio, Intermediates in wet oxidation of cellulose: identification of hydroxyl radical and characterization of hydrogen peroxide, Water Res. 36 (2002) 4821–4821.

[15] S.K. Kolaczkowski, P. Plucinski, F.J. Beltran, F.J. Rivas, D.B. McLurgh, Wet air oxidation: a review of process technologies and aspects in reactor design, Chem. Eng. J. 73 (1999) 143–160.

[16] F.J. Zimmerman, D.G. Diddams, The Zimmerman process and its applications in the pulp and paper industry, Tappi 43 (1960) 710–715.

[17] W. Tang, X. Zeng, J. Zhao, G. Gu, Y. Li, Y. Ni, The study on the wet air oxidation of highly concentrated emulsified wastewater and its kinetics, Sep. Purif. Technol. 31 (2003) 77–82.

[18] V.S. Mishra, V.V. Mahajani, J.B. Joshi, Wet air oxidation, Ind. Eng. Chem. Res. 34 (1995) 2–48.

[19] L. Oliviero, J.J. Barbier, D. Duprez, A. Guerrero-Ruiz, B. Bachiller, R.I. Ramos, Catalytic wet air oxidation of phenol and acrylic acid over Ru/C and Ru–CeO$_2$/C catalysts, Appl. Catal. B 25 (2000) 267–275.

[20] D. Himmelblau, Solubilities of inert gases in water 0 °C to near the critical point of water, J. Chem. Eng. Data 5 (1960) 10.

[21] H. Debellefontaine, J.N. Foussard, Wet air oxidation for the treatment of industrial wastes. Chemical aspects, reactor design and industrial applications in Europe, Waste Manage. 20 (2000) 15–25.

[22] J. Rivas, S.T. Kolaczkowski, F.J. Beltran, D.B. McLurgh, Degradation of maleic acid in a wet air oxidation environment in the presence and absence of a platinum catalyst, Appl. Catal. B 22 (1999) 279–291.

[23] Y. Kaçar, E. Alpay, V.K. Ceylan, Pretreatment of Afyon alcaloide factory's wastewater by wet air oxidation (WAO), Water Res. 37 (2003) 1170–1176.

[24] M. Jeworski, E. Heinzle, Combined chemical–biological treatment of wastewater containing refractory pollutants, Biotechnol. Annu. Rev. 6 (2000) 163–196.

[25] D.H. Volman, J.R. Seed, The photochemistry of uranyl oxalate, J. Am. Chem. Soc. 86 (1964) 5095–5098.

[26] W.J. Weber, Physicochemical Processes for Water Quality Control, Wiley/Interscience, New York, 1972.

[27] I. Arslan-Alaton, I.A. Balcioglu, Photochemical and heterogeneous photocatalytic degradation of waste vinylsulphone dyes: a case study with hydrolyzed Reactive Black 5, J. Photochem. Photobiol. A 141 (2001) 247–254.

[28] SO 10712-1995-12-15, 1995. Water Quality–*Pseudomonas putida* Growth Inhibition Test (*Pseudomonas* Cell Multiplication Inhibition Test), 1st ed., ISO, Geneve, Switzerland.

[29] D. Chen, A.K. Ray, Photodegradation kinetics of 4-nitrophenol in TiO$_2$ suspension, Water Res. 32 (1998) 3223–3234.

[30] V. Augugliaro, M.M.J. Lopez, L. Palmiaro, Influence of pH on the degradation kinetics of nitrophenol isomers in a heterogeneous photocatalytic system, J. Soria, Appl. Catal. A 101 (1993) 7–13.

[31] S. Sakthivel, B. Neppolian, M.V. Shankar, B. Arabindoo, M. Palanichamy, V. Murugesan, Solar photocatalytic degradation of azo dye: comparison of photocatalytic efficiency of ZnO and TiO$_2$, Solar Energy Mater. Solar Cells 77 (2003) 65–82.

[32] M.S. Vohra, K. Tanaka, Enhanced photocatalytic activity of Nafion-coated TiO$_2$, Environ. Sci. Technol. 35 (2001) 411–415.

[33] N. Daneshvar, D. Salari, A.R. Khataee, Photocatalytic degradation of azo dye acid red 14 in water: investigation of the effect of operational parameters, J. Photochem. Photobiol. A 157 (2003) 111–116.

[34] A.M. Peiró, J.A. Ayllón, J. Peral, X. Doménech, TiO$_2$-photocatalyzed degradation of phenol and *ortho*-substituted phenolic compounds, Appl. Catal. B 30 (2001) 359–373.

[35] J.B. Heredia, J. Torregrosa, J.P. Dominguez, J.A. Peres, Oxidation of *p*-hydroxybenzoic acid by UV radiation and by TiO$_2$/UV radiation: comparison and modelling of reaction kinetic, J. Hazard. Mater. B 83 (2001) 255–264.

[36] G. McKay, H.S. Blair, J.R. Gardner, Adsorption of dyes on chitin. I. Equilibrium studies, J. Appl. Polym. Sci. 27 (1982) 3043–3057.

[37] G. Chen, L. Lei, X. Hu, P.L. Yue, Kinetic study into the wet air oxidation of printing and dyeing wastewater, Sep. Purif. Technol. 31 (2003) 71–76.